Hindawi
Mathematical Problems in Engineering
Volume 2018, Article ID 2161937, 9 pages
https://doi.org/10.1155/2018/2161937

Research Article

An Energy Efficient Two-Stage Supply Pressure Hydraulic System for the Downhole Traction Robot

Delei Fang, Jianzhong Shang, Junhong Yang, Zhuo Wang, Yong Xue, and Wei Wu

College of Mechatronic Engineering and Automation, National University of Defense Technology, Changsha 410073, China

Correspondence should be addressed to Jianzhong Shang; jz_shang_nudt@163.com

Received 12 December 2017; Revised 3 May 2018; Accepted 20 May 2018; Published 11 June 2018

Academic Editor: Anna M. Gil-Lafuente

The efficiency of hydraulic drive system has become one of the significant issues in mobile robot. In this paper, an energy efficient two-stage supply pressure hydraulic system is proposed to solve the energy waste in the one-stage supply pressure system of the downhole traction robot. This novel two-stage hydraulic system can match different pressure requirements of actuator by changing the modes of supply pressure, which is helpful to reduce the energy loss and improve the efficiency for traction robot. Based on the robot working principle, the load characteristics in different actuators are obtained and the shortage in traditional hydraulic system is analyzed. The novel hydraulic system which consists of a high-pressure source and a low-pressure source is designed, including the system structure and energy supply method. According to the energy flow process, energy loss models of the system and components are established to analyze energy-saving principle of the novel hydraulic system. The feasibility and efficiency of two-stage supply pressure system are verified by simulating the operating process of telescopic mechanism. Finally, the simulation shows that control precision of the novel system can reach 3.5 mm and the efficiency is increased to 59.53%, which can provide theoretical reference for design of hydraulic drive system in traction robot and the efficiency improvement of multiactuator mobile robot.

1. Introduction

With the development of information technology, sensation technology, and control technology, mobile robots have been dramatically improved, which can be widely used in military, industry, and civil service [1–3]. As a kind of mobile robots, downhole traction robots have been applied to the development in petroleum field in recent years. Also, they play an important role in well drilling, logging, and other borehole operations [4, 5]. In order to raise load capacity, more and more traction robots are using hydraulic system. However, most traditional systems have the shortcomings of low drive efficiency and large heat release, which severely affect the reliability and durability in the robot operation [6–8].

Traction robot works in the complex environment with high temperature and high pressure. While, if the energy consumption is large in the narrow pipe, there will be lots of problems.

(1) The high energy loss requires the system to have higher power, so the high power motor and pump should be chosen, which inevitably leads to the increase of weight and volume of motor and pump.

(2) When the robot performs lower power action, it will inevitably result in a lot of pressure drop loss, which dissipates in the form of heat.

(3) As the energy loss increases, the system becomes more heated, the power of the cooling system should be larger, and volume and weight of the cooling system increases, which will also affect the compact structure of the robot.

(4) If the heat is not dissipated timely, it will affect the normal operation of relevant machine components, which inevitably affect robot working safety.

Therefore, improving the drive efficiency of hydraulic system has become one of the most essential techniques to develop downhole traction robot.

So far, the research of downhole traction robot has been focused on mechanical design, trajectory planning, and stability control. However, there are few studies on the efficiency of hydraulic drive systems. We can refer to the research on efficiency of mobile robot hydraulic power unit in recent years [9–11].

Helmut Kogler proposes a new type of hydraulic buck converter consisting of high frequency switch valves, elongated tubes, and accumulators, which can enhance the system efficiency by matching output pressure with the requirements of actuator. However, the thin pipe which is used as an inertial device is too long to be placed in the limited space of robot. In addition, the pressure wave in the elongated pipe affects the converter's ability to adjust the pressure and reduces the energy utilization [12–14]. Kyoung Kwan Ahn designs a device to achieve energy recovery and release, which consists of a flywheel, hydraulic motor, and a large capacity accumulator [15, 16]. Due to the limitation of volume and weight, this method is mainly applied in excavators, vehicles, and other large equipment, which is not available for traction robot. Now, there are also applications of two-stage power supply applied to hydraulic press and hydraulic lift machinery, whose idea of saving energy is to reuse excessive energy. When the machine operates, the extra potential energy is stored in the accumulator. When the machine runs again, the extra potential energy is released from the accumulator, to improve the power system energy efficiency. However, this method does not solve the problem of excessive energy output primarily [17, 18].

Beside the devices which are attached to the system to improve the efficiency, some special control method is developed to reduce energy loss [19, 20]. A. R. Plummer and D. N. Johnston put forward a variable pressure control method called VPVC (variable supply pressure valve-controlled). The method can predict the load and adjust the speed of motor, which can make system pressure match the pressure required for the actuator. This method can reduce throttling loss at control valve. However, the system pressure only matches the maximum pressure of the actuators in operation. For other actuators, there is still much energy loss due to excessive input pressure. Monika Ivantysynova proposed removing proportional control valve and control motor speed to adjust output flow rate, which can directly dominate the movement of hydraulic cylinder. So, this method achieves high efficiency due to the elimination of throttling loss caused by excess flow [21–24]. However, this method requires that each actuator must be configured with one pump and one motor, resulting in a large hydraulic system, which is not suitable for small mobile robots.

In view of the traction robot characteristics of complex dynamic performance in multiactuators and compact mechanical structure, the previous energy-saving methods are not applicable to downhole traction robot hydraulic system. In this paper, a novel two-stage supply pressure hydraulic system is proposed, which can make system pressure match the requirement of actuator, reduce throttling loss in servo valve, and improve the efficiency of the hydraulic system of downhole traction robot. Based on the traction robot working principle, the loads of all actuators are analyzed. Then mechanism structure and operating principle of two-stage supply pressure hydraulic system are presented. According to the energy flow process in the robot, energy loss models in traditional system and the novel system are established, which can be used to analyze the energy-saving reason in the novel system relative to the traditional one. Finally, telescopic mechanism is selected as an example to analyze efficiency of two-stage supply pressure system. And operating process in the novel system is simulated, which can be used to prove feasibility and energy-saving in two-stage supply pressure system. The novel pressure supply method is different from the existing application, mainly in the mode of energy supply and energy-saving idea. The purpose of this paper is to provide reference and guidance for practical design for traction robot hydraulic system and mathematical analysis on drive efficiency for multiactuator mobile robot.

2. Mechanism and Design of Two-Stage Supply Pressure Hydraulic System

2.1. Working Principle of Downhole Traction Robot. Figure 1 shows downhole traction robot (or DTR, for short) based on the single-directional locking mechanism, which consists of two locking mechanisms and one telescopic mechanism[25]. Locking function and horizontal motion are realized separately by the asymmetric hydraulic actuators, and hydraulic system of the traction is shown in Figure 2. DTR traditionally adopts the supply mode of one-stage supply pressure, which is that a pump is driven by a motor to supply pressure for all hydraulic actuators. At present, the energy supply for the driving motor is realized by cable, which is connected to the ground.

As shown in Figure 1, DTR assembles drill bits and other underground equipment on the right end, which is selected as the forward direction. In the initial state, as shown in Figure 1(a), the locking arm shrinks and the DTR remains static. In the working step 1 which is shown in Figure 1(b), pressed oil enters small cavity (or the cavity with rod) of locking actuator 2. Pressed oil drives piston rod to move, which pushes locking arm and locking wheel to lock the pipe. The pressed oil enters big cavity (or the cavity with no rod) of telescopic actuator and pushes bit for drilling operation. As telescopic piston moves one stroke, locking mechanism 1 begins to lock the hole and locking mechanism 2 shrinks the hole. The pressed oil enters small cavity of telescopic actuator and the rear part of DTR is dragged forward, as shown in Figure 1(c). After movement is accomplished, DTR is back to the state in Figure 1(a). So DTR can realize motion by repeating motions from Figures 1(a)–1(c).

As shown in Figure 2, traditional hydraulic system of DTR is a one-stage supply pressure system (or OSP, for short). In order to ensure that all actuators work properly, the maximum pressure required in all actuators must be selected as system output pressure. However, each actuator requires different pressures in different operating modes. Also, at different times, the pressure required in one actuator varies greatly.

The clamping force is mainly related to the friction force of pipe, which is a complicated physical quantity and difficult to measure. The clamping data is obtained through

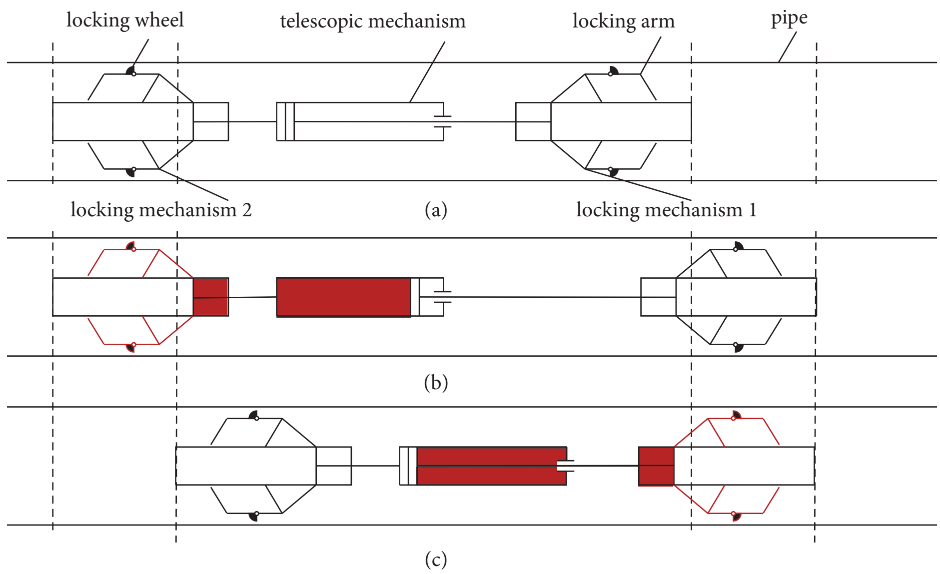

FIGURE 1: Schematic diagram of traction robot motion.

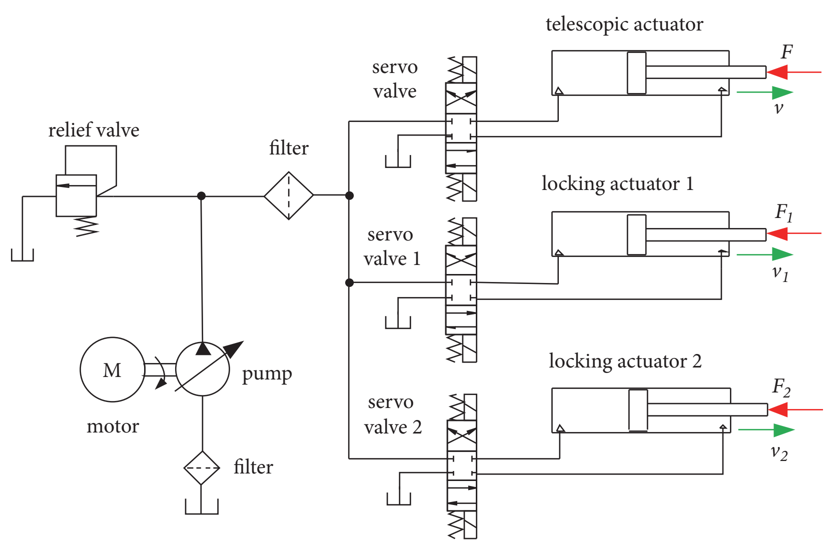

FIGURE 2: Diagram of downhole traction robot hydraulic system.

simulation based on ADAMS and AMESim. In fact, during operation the forces will fluctuate. To simplify simulation research, all the forces are rounded into integers. As shown in Figure 3, the load forces of all actuators under drilling operation mode are depicted. The load force of telescopic actuator is the most severe, which can vary from -300N to 6500N, while load range of supporting actuator 1 is -600N to 1500N and load range of supporting actuator 2 is -300N to 3000N.

According to the above analysis, to make sure the robot can operate, output pressure in traditional OSP hydraulic system must match the maximum load 6500N, which has exceeded the pressure requirement of other actuators. Therefore, to meet the needs of small load in other actuators, the redundant output pressure for actuator should be lost in throttling form at the corresponding servo valve. The lost energy is converted into heat, not only reducing the energy efficiency of hydraulic system but also affecting the reliability of DTR.

2.2. Design of Two-Stage Supply Pressure Hydraulic System. During the DTR operation, load force of actuator changes dramatically and the duration of peak value is relatively short. Combined with the above traction features, a novel energy efficient two-stage supply pressure hydraulic system is presented in this paper, which is abbreviated as TSP. TSP hydraulic system has a low-pressure source and an instantaneous high-pressure source including a switch valve and a small accumulator. As shown in Figure 4, the low-pressure pump is responsible for low-pressure supply of three actuators, and the high-pressure pump is used to charge energy for accumulator. The low-pressure pump is connected

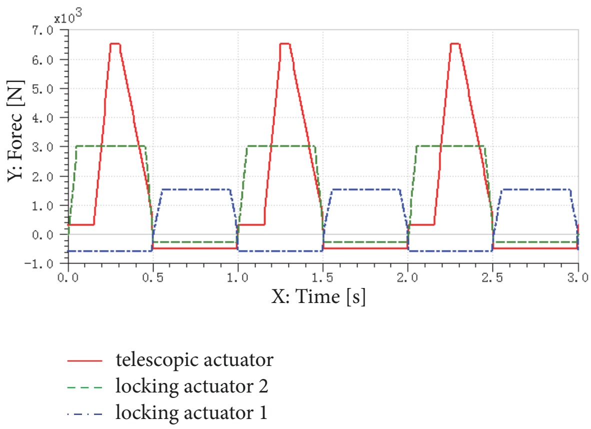

Figure 3: Load curves on actuators under drilling mode.

directly to the motor, while the high-pressure pump is connected with the motor through the clutch. When received signal that the accumulator pressure arrives presets pressure value, the control system issues instruction to separate the high-pressure pump from motor. Otherwise the control system sends instructions to connect the high-pressure pump with the motor to replenish energy to accumulator.

According to the working principle, traction robot movement is driven by three actuators. Because of low-pressure requirement, the two supporting actuators can be driven by low-pressure source. To meet the high-pressure demand, telescopic actuator is offered pressure by low-pressure source and a small auxiliary high-pressure accumulator. When the load on telescopic mechanism is small, telescopic actuator is supplied by the low-pressure source. When the load becomes so large that the low-pressure source cannot meet, telescopic actuator is transformed into high-pressure supply mode by opening switch valve.

When DTR is operating normally, the load force has a very short peak value and the pressures of two supporting actuators both are far less than the peak load value. So, driving three actuators by the OSP system leads to a large number of throttling losses inevitably. TSP system can offer different actuators different pressures, according to the different load forces. Therefore, the TSP method can reduce throttling loss resulting from redundant pressure of OSP in a long time, which can increase energy efficiency of fluid power system in the robot.

3. Energy Loss Analysis of Two Hydraulic Systems

In the research on traction robot and pipeline robot, many scholars focus on structural design and stability design and there is little research on energy consumption of power system. Therefore, the establishment and analysis of mathematical model for energy-saving will provide theoretical reference for the research on mobile robot power system.

Energy loss models are established to explain the reason why efficiency of TSP system is higher than that of OSP system. In order to research the different effects of two hydraulic systems on robot efficiency, we do not consider transmission energy loss between motor and pump and output energy loss of pump. The energy loss in the switch valve is ignored because of large opening and minute pressure drop. In the two types of hydraulic system, robot performs the same amount of work and actuators need the same power.

3.1. Energy Loss Models of Systems. The balance equation of power in OSP system is expressed as

$$P_{in} = P_{pi} + P_{va} + P_{cy} + P_{out} \tag{1}$$

where P_{in} is the total input power. P_{pi} is the power loss in the fluid pipe. P_{va} is the power loss in the servo valve. P_{cy} is the power loss of hydraulic cylinder. P_{out} is the total output power.

For OSP, by assuming that T is the operating time, the total energy transmission loss of hydraulic system during a period is expressed as

$$E_{de} = \int_0^T \left(P_{pi} + P_{va} + P_{cy}\right) dt \tag{2}$$

Similarly, power loss for TSP system is expressed as

$$P'_{in} = P^{(1)}_{pi} + P^{(2)}_{pi} + P^{(2)}_{ac} + P'_{va} + P'_{cy} + P'_{out} \tag{3}$$

where P'_{in} is the total input power, P'_{out} is the total output power, and P'_{va} is the power loss in servo valve. P'_{cy} is the power loss of hydraulic cylinder. In high-pressure supply circuit, $P^{(2)}_{pi}$ is the power loss in the fluid pipe and $P^{(2)}_{ac}$ is the power loss in the accumulator. In low-pressure supply circuit, the power loss in the fluid pipe *is* $P^{(1)}_{pi}$.

For TSP, the total energy transmission loss of hydraulic system is expressed as

$$\begin{aligned} E'_{de} = {} & \int_0^{T_1} P^{(1)}_{pi} dt + \int_0^{T_2} \left(P^{(2)}_{pi} + P^{(2)}_{ac}\right) dt + \int_0^T P'_{va} dt \\ & + \int_0^T P'_{cy} dt \end{aligned} \tag{4}$$

where T1 is the time of low-pressure energy supply and T2 is the time of high-pressure energy supply. To analyze the specific energy loss difference between the two systems, paper establishes energy loss in fluid pipe, energy loss in accumulator, and energy loss in actuator including the servo valve and the cylinder.

3.2. Energy Loss in Fluid Pipe. Because the pressure in the two systems is different, it is necessary to analyze whether the loss in fluid pipe is also different. It is assumed that dimensions of all pipes are the same. The loss pressure along pipe is expressed as

$$\Delta p = \lambda \frac{l}{2} \frac{\rho v^2}{d} \tag{5}$$

where λ is pipe friction coefficient, ρ is fluid density, v is the liquid velocity in pipe, l is pipe length, and d is the inner diameter of pipe.

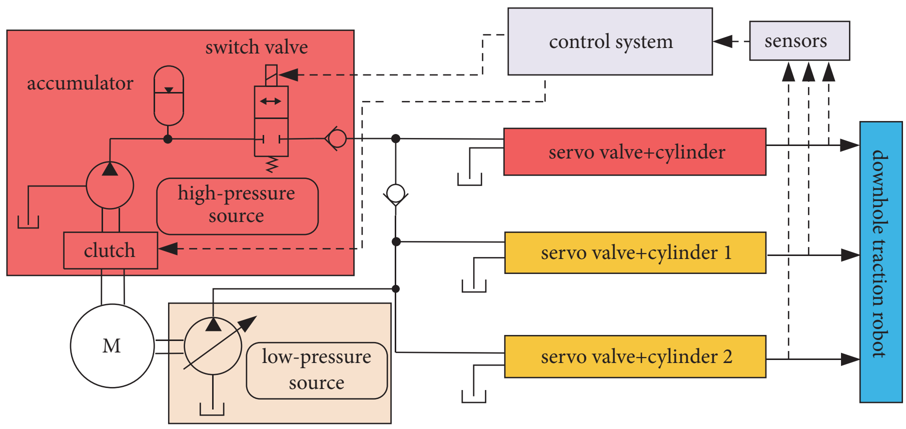

FIGURE 4: Schematic diagram of two-stage supply pressure system.

When flow rate through the pipe is q, the relationship between flow rate and liquid velocity can be obtained:

$$v = \frac{q}{S} = \frac{4}{\pi}\frac{q}{d^2} \tag{6}$$

By combining (5) and (6), the pipe power loss is expressed as

$$\begin{aligned} P_{pi} &= \Delta p_{pi} \cdot q_{pi} = \lambda \frac{8}{\pi^2}\frac{{q_{pi}}^3}{d^5} l_{pi}\rho \\ P_{pi}^{(1)} &= \Delta p_{pi}^{(1)} \cdot q_{pi}^{(1)} = \lambda \frac{8}{\pi^2}\frac{\left[q_{pi}^{(1)}\right]^3}{d^5} l_{pi}^{(1)}\rho \\ P_{pi}^{(2)} &= \Delta p_{pi}^{(2)} \cdot q_{pi}^{(2)} = \lambda \frac{8}{\pi^2}\frac{\left[q_{pi}^{(2)}\right]^3}{d^5} l_{pi}^{(2)}\rho \end{aligned} \tag{7}$$

where q_{pi} is flow rate in the OSP, $q_{pi}^{(1)}$ is the flow rate in the low-pressure circuit of the TSP, $q_{pi}^{(2)}$ is the flow rate in the high-pressure circuit, l_{pi} is pipe length of the OSP, $l_{pi}^{(1)}$ is the length of the low-pressure circuit, and $l_{pi}^{(2)}$ is the length of the high-pressure circuit.

During one cycle, the difference of pipe power loss in OSP and TSP is expressed as

$$\Delta E_{pi} = \int_0^T P_{pi} dt - \int_0^{T_1} P_{pi}^{(1)} dt - \int_0^{T_2} P_{pi}^{(2)} dt \tag{8}$$

Obviously, when actuator operates the same motion, the required flow rates are identical in the both systems. And, l_{pi} and $l_{pi}^{(1)}$ have the same length; combining (7) and (8), the energy loss dissipation is obtained.

$$\Delta E_{pi} = \lambda \frac{8\rho}{\pi^2 d^5}\left(l_{pi} - l_{pi}^{(2)}\right)\int_0^{T_2} {q_{pi}^{(2)}}^3 dt \tag{9}$$

Assuming that l_{pi} and $l_{pi}^{(2)}$ are the same length, the value of (9) is zero. Therefore, pipe power loss in the two systems will be the same, despite the different system pressures.

3.3. Energy Loss in Accumulator. It is also essential to analyze power loss in accumulator, as the accumulator is the important component in TSP. When gas is compressed, heat is generated and the energy is lost, which is irreversible in the system. The energy loss in accumulators is expressed as

$$\begin{aligned} \Delta E_{ac} &= \int_0^{T_0} P_c^{(1)} dt - \int_0^{T_2} P_d^{(2)} dt \\ &= \int_0^{T_0} p_c^{(1)}(t)\, q_c^{(1)}(t)\, dt \\ &\quad - \int_0^{T_2} p_d^{(2)}(t)\, q_d^{(2)}(t)\, dt \end{aligned} \tag{10}$$

$$\int_0^{T_0} q_c^{(1)}(t)\, dt = \int_0^{T_2} q_d^{(2)}(t)\, dt \tag{11}$$

where $q_c^{(1)}$ is the flow rate streaming into the accumulator, $q_d^{(2)}$ is the flow rate issuing from the accumulator, $p_c^{(1)}$ is the pressure in energy storage, $p_d^{(2)}$ is the pressure in energy releasing state, and T_0 is the energy recharging time.

3.4. Energy Loss in Actuator. As shown in Figure 5, the actuator includes servo valve and hydraulic cylinder. The energy loss in actuator is the main loss in hydraulic system. The reason is that input pressure provided in hydraulic system is greater than the pressure required by the load, which causes redundant pressure to be wasted in the form of throttling loss at servo valve. Therefore, reducing throttling loss is the main reason that TSP system is more efficient than OSP system.

The mathematical model of power loss in actuator is obtained. The balance equation of power is expressed as follows:

$$P_{in0} = P_{vat} + P_{vab} + P_{cy} + P_{out} \tag{12}$$

$$P_{va} = P_{vat} + P_{vab} \tag{13}$$

where P_{in0} is the input power, P_{vat} is the throttling loss at the inlet, and P_{vab} is the throttling loss at the outlet.

There is a force equilibrium equation in cylinder.

$$p_1 A_{in} - p_2 A_{out} = F_{load} + m x'' \tag{14}$$

Table 1: Simulation parameters in hydraulic system.

parameter	value
The diameter of cylinder piston (m)	0.024
The diameter of cylinder rod (m)	0.012
The length of the stroke (m)	0.1
The servo valve natural frequency (Hz)	100
The switch valve natural frequency (Hz)	50
The maximal flow rate of low-pressure pump (L/min)	60
The maximal flow rate of high-pressure pump (L/min)	10
The maximal pressure of the low-pressure pump (MPa)	7.5
The maximal pressure of the high-pressure pump (MPa)	21
The gas precharge pressure (MPa)	18
The polytropic index	1.2
The accumulator volume (L)	0.2

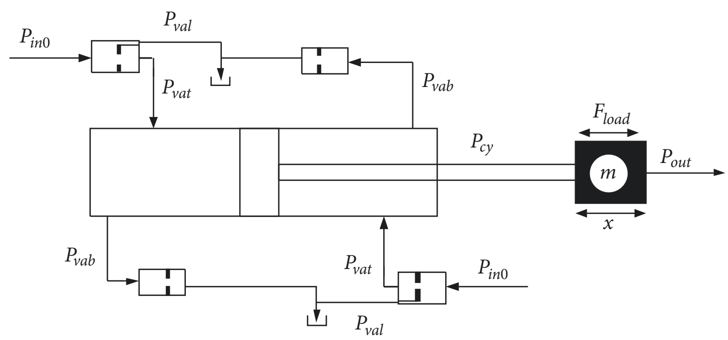

Figure 5: Schematic diagram of power flow in actuator.

where F_{load} is the load force, m is the total mass, x is the piston displacement, A_{in} is the area of cylinder piston, A_{out} is the area in cavity of no rod, p_1 is the pressure of filling chamber, and p_2 is the pressure of returning chamber.

At servo valve port, the fluid flow equation is obtained

$$q_{in} = A_{in}x' = C_d A_0 \sqrt{\frac{2(p_{in} - p_1)}{\rho}}$$
$$q_{out} = A_{out}x' = C_d A_0 \sqrt{\frac{2p_2}{\rho}} \tag{15}$$

where C_d is the metering coefficient and A_0 is the sectional area of the orifice.

Through formulas (14) and (15), the throttling loss power in servo valve can be calculated

$$P_{vat} = (p_{in} - p_1) \cdot q_1 = \frac{A_{in}^3 x'}{A_{in}^3 + A_{out}^3}\left(p_{in}A_{in} - F_{load} - mx'\right) \tag{16}$$

$$P_{vab} = p_2 \cdot q_2 = \frac{A_{out}^3 x'}{A_{in}^3 + A_{out}^3}\left(p_{in}A_{in} - F_{load} - mx'\right) \tag{17}$$

As shown in formulas (16) and (17), on the premise other parameters are constant. The two equations reveal the relationship between input pressure and throttling loss that the input pressure is higher and the throttling loss is larger.

In TSP system, the pressure of charging gas is not lower than the maximum load on actuators, so the output pressure of accumulator is higher than the system pressure in OSP system. By combining (14), (15), (16), and (17), saved energy at servo valve is expressed as follows:

$$\Delta E_{va} = \int_0^{T_1} \left(p_0 - p_0^{(1)}\right) A_{in}x'dt - \int_0^{T_2} \left(p_0^{(2)} - p_0\right) A_{in}x'dt \tag{18}$$

Based on the above analysis, the energy saved in TSP system is got.

$$\Delta E_{de} = E_{de} - E'_{de} = \Delta E_{va} - \Delta E_{ac} \tag{19}$$

4. Simulation and Discussion

In order to verify the feasibility and energy-saving of TSP hydraulic system, simulation analyses of TSP system and OSP system are carried out based on AMESim. Telescopic mechanism of traction robot is selected as the simulation object; the same load and displacement are used as the simulation inputs in the two hydraulic systems. According to the robot motion characteristics and working principle of hydraulic system, the simulation parameters are set as shown in Table 1. In order to meet the requirements of high-pressure supply (the working time is from 0.2s to 0.4s) and linear output pressure, the frequency of switch valve is set to 50Hz.

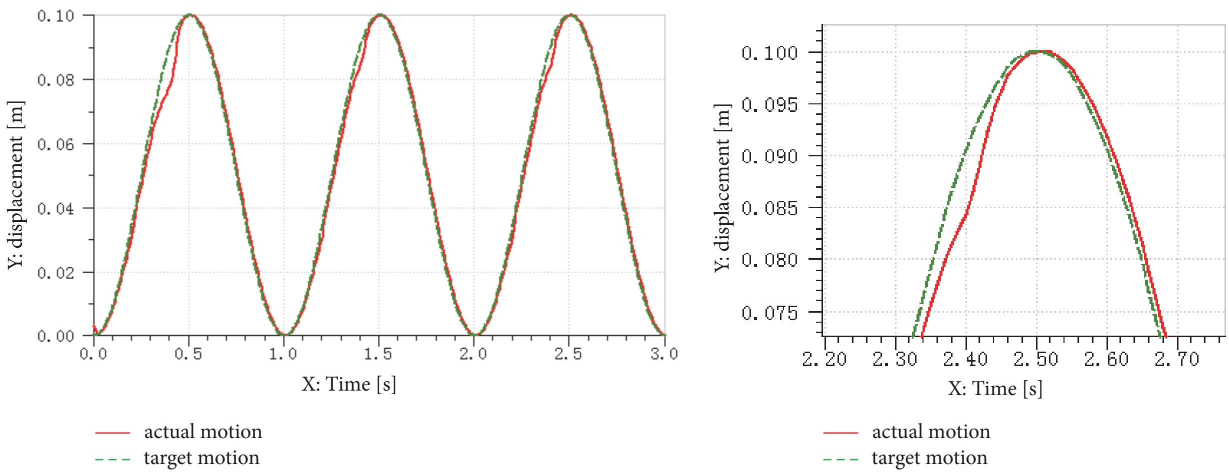

(a) (b)

Figure 6: Displacement tracking curve of the actuator driven by TSP system.

The input displacement in simulation is the ideal sinusoidal signal, whose frequency is 1Hz and amplitude is 0.1m. The input load of hydraulic actuator is depicted in Figure 2. The output displacement curve of telescopic mechanism under TSP system is obtained, as shown in Figure 6.

As shown in Figure 6(a), TSP hydraulic system can drive the actuator move according to the displacement planning, the control accuracy can reach 3.5 mm, and the time delay is 0.05 s, which can meet the movement requirements of traction robot. It can be seen from Figure 6(b) that piston movement fluctuates at the moment of high frequency switch valve opening, which is the moment when the accumulator releases the oil, caused by the insufficient flow instantaneously. In order to avoid fluctuating, some measures should be taken, such as before switch valve opens; servo valve opening size should be adjusted in advance to stabilize input pressure and flow.

Then, the output pressures of two systems are analyzed and pressure curves simulated are shown in Figure 7.

It can be seen from the graph that system pressure supplied by one-stage system is constant 16MPa. The system pressure provided by two-stage system is variable. The output pressure maintains at a low level in the most times and, when the larger driving force is needed, the output pressure is higher than that of one-stage system. Therefore, in actuator operation especially the low driving force is needed; OSP system produces a greater pressure loss at the inlet of servo valve than TSP system.

In order to directly observe the energy consumption difference between two pressure supply systems, output power curves are obtained, as shown in Figure 8.

It can be seen clearly from Figure 8 that the output power of TSP system is lower than the output power of OSP system in most working times. Only in the moment when actuator has a high load force, which represents accumulator starting to work, is the output power of TSP system larger than the output power of OSP system. While, for the whole working time, the high-pressure energy supply is very short. Therefore,

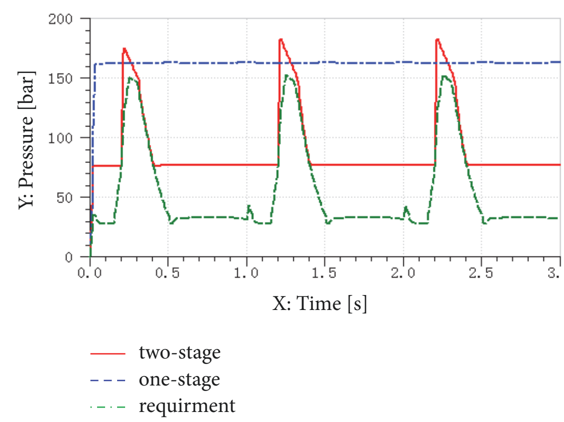

Figure 7: Pressure curves of two pressure supply systems.

the power loss in two-stage supply pressure system is much lower than the power loss in one-stage supply pressure system.

Based on the power curves and the previous formulas, the total energy consumption of the two systems can be calculated, as shown in Figure 9.

In Figure 9, the green dashed line describes the actual energy required for telescopic actuator, the red solid line describes the energy consumption in two-stage supply pressure system, and the blue dotted line is the energy consumption in one-stage energy supply system. As can be seen from Figure 9, the actual energy required for telescopic actuator in three periodic motions is 1193J. When actuator operates under the OSP system, the total energy consumed is 3461J. When actuator operates under the TSP system, the total energy consumed is 2004J. Therefore, the efficiency of OSP system is 34.47%, while the efficiency of TSP system is 59.53%, which is increased by 25.06%.

At the same time, the total energy consumption of all hydraulic components in the two pressure systems is

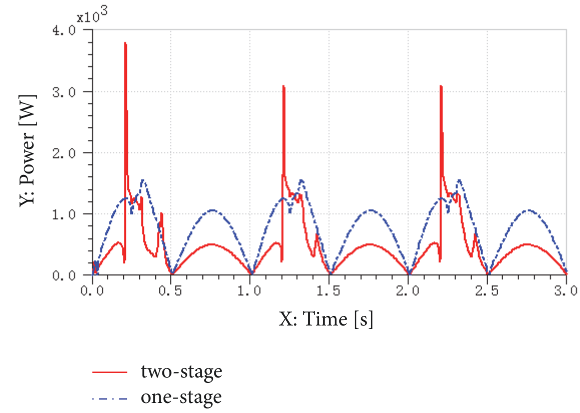

FIGURE 8: Output power curves of two pressure supply systems.

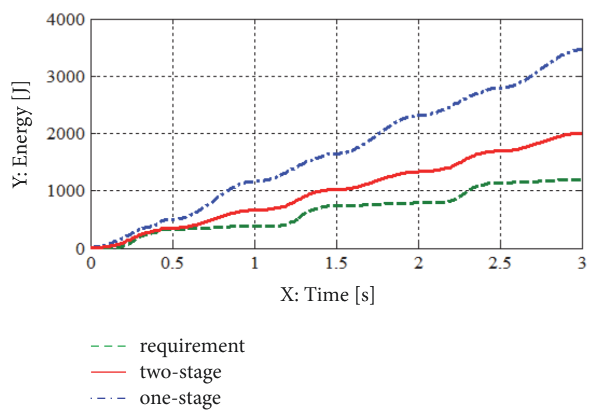

FIGURE 9: Energy consumption curves in two systems.

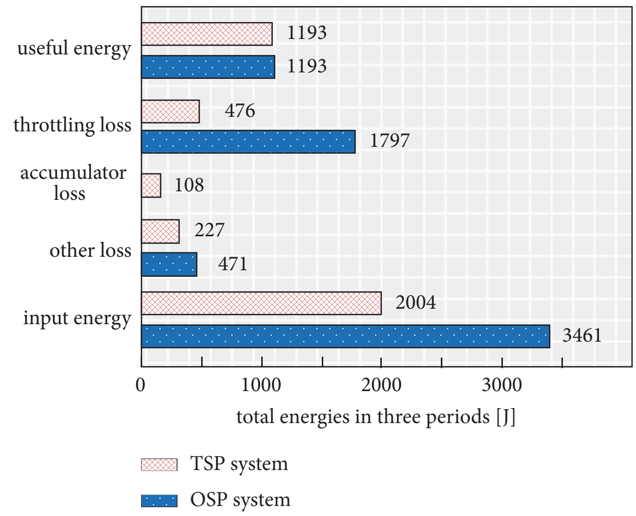

FIGURE 10: The bars chart of energy consumption in hydraulic components.

calculated and the bars chart of energy consumption is shown in Figure 10.

As shown in Figure 10, under the same load conditions, if two-stage hydraulic system is adopted, the throttling loss of the servo valve is much smaller than that of traditional hydraulic system. Because of the accumulator, the added energy loss is 108J. The loss is tiny relative to throttle loss. So, reducing throttling loss is the main reason why the novel two-stage supply pressure system is highly efficient.

5. Conclusions

Based on the working principle of downhole traction robot, the load characteristics of three actuators are obtained. In view of the reason for the throttling loss in the one-stage supply pressure hydraulic system, a novel two-stage supply pressure hydraulic system is proposed, which can improve driving efficiency through different pressure supply modes.

The energy loss model of traction robot hydraulic system and the significant components were established, and the specific forms and mathematical expressions were obtained, which is helpful to analyze the energy-saving principle and design the component in the novel hydraulic system

The feasibility of two-stage supply pressure hydraulic system is verified by simulation. The results have shown that the control accuracy can reach 3.5 mm and the time delay is 0.05s, which can meet the movement requirements of downhole traction robot.

Based on simulation data and formulas, the power and energy consumed in the two types of drive system were obtained, which has shown that the efficiency in two-stage supply pressure system can be increased to 59.53%. The main reason why two-stage system can improve efficiency is reducing the much throttling loss at servo valve.

Conflicts of Interest

The authors declare no conflicts of interest.

Acknowledgments

The work reported in this paper was supported by the National Natural Science Foundation of China (nos. 51675527, 51675522).

References

[1] T. Li, S. Ma, B. Li, M. Wang, and Y. Wang, "Axiomatic design method to design a screw drive in-pipe robot passing through varied curved pipes," *Science China Technological Sciences*, vol. 59, no. 2, pp. 191–202, 2016.

[2] L. I. Yujia, Q. Liu, Y. Chen, and T. Ren, "Design and analysis of an active helical drive downhole traction," *Chinese Journal of Mechanical Engineering*, vol. 30, pp. 1–10, 2017.

[3] T. Li, S. Ma, B. Li, M. Wang, and Y. Wang, "Fuzzy theory based control method for an in-pipe robot to move in variable resistance environment," *Chinese Journal of Mechanical Engineering*, vol. 28, no. 6, pp. 1213–1221, 2015.

[4] I. Ahmad, O. Akimov, P. Bond et al., “Reliable technology for drilling operations in a high-pressure/high- temperature environment,” in *Proceedings of the SPE/IADC Drilling Conference and Exhibition 2014*, pp. 500–515, March 2014.

[5] F. Frans, A. Cuauro, E. Chalco, D. Brink, M. Ghozali, and N. Bounoua, “Tractor production logging in long cased horizontal wells; operational experience from the Al Shaheen field, Offshore Qatar,” in *Proceedings of the International Petroleum Technology Conference 2014 - Innovation and Collaboration: Keys to Affordable Energy, IPTC 2014*, pp. 2745–2755, December 2014.

[6] T. Sheiretov, “Wireline tractors and mechanical services tools: Comparative study of technical solutions,” in *Proceedings of the SPE/ICoTA Coiled Tubing and Well Intervention Conference and Exhibition 2016*, March 2016.

[7] D. Heddleston, “An evaluation of well deployment aspects affecting well flow performance on horizontal production log results,” in *Proceedings of the Coiled Tubing and Well Intervention Conference and Exhibition 2013*, pp. 571–579, March 2013.

[8] Y. Li, Q. Liu, and W. Li, “Development of a novel oil and gas in-pipe robot,” *International Journal of Mechatronics & Manufacturing Systems*, vol. 8, article 102, 2015.

[9] X. Ouyang, S. Ding, B. Fan, P. Y. Li, and H. Yang, “Development of a novel compact hydraulic power unit for the exoskeleton robot,” *Mechatronics*, vol. 38, pp. 68–75, 2016.

[10] H. Yang and M. Pan, “Engineering research in fluid power: a review,” *Journal of Zhejiang University-SCIENCE A*, vol. 16, no. 6, pp. 427–442, 2015.

[11] G. Altare and A. Vacca, “A Design Solution for Efficient and Compact Electro-hydraulic Actuators,” in *Proceedings of the 2nd International Conference on Dynamics and Vibroacoustics of Machines, DVM 2014*, pp. 8–16, September 2014.

[12] H. Kogler and R. Scheidl, “Linear motion control with a low-power hydraulic switching converter - Part I: Concept, test rig, simulations,” *Proceedings of the Institution of Mechanical Engineers, Part I: Journal of Systems and Control Engineering*, vol. 229, no. 8, pp. 677–684, 2015.

[13] H. Kogler and R. Scheidl, “Energy efficient linear drive axis using a hydraulic switching converter,” *Journal of Dynamic Systems, Measurement, and Control*, vol. 138, no. 9, 2016.

[14] H. Kogler, R. Scheidl, and M. Ehrentraut, “A simulation model of a hydraulic buck converter based on a mixed time frequency domain iteration,” in *Proceedings of the ASME/BATH 2013 Symposium on Fluid Power and Motion Control, FPMC 2013*, pp. 1–6, October 2013.

[15] H. H. Triet and K. K. Ahn, “Comparison and assessment of a hydraulic energy-saving system for hydrostatic drives,” *Proceedings of the Institution of Mechanical Engineers, Part I: Journal of Systems and Control Engineering*, vol. 225, no. 1, pp. 21–34, 2011.

[16] T. H. Ho and K. K. Ahn, “Modeling and simulation of hydrostatic transmission system with energy regeneration using hydraulic accumulator,” *Journal of Mechanical Science and Technology*, vol. 24, no. 5, pp. 1163–1175, 2010.

[17] H. Yang, D. Hu, and B. Xu, “Energy-saving technology of variable counterweight and its energy consumption analyses,” *Journal of Mechanical Engineering*, vol. 46, no. 2, pp. 132–138, 2010.

[18] J. Yao, B. Li, and X. Kong, “Energy saving and control of hydraulic press fast forging system based on the two-stage pressure source,” *Journal of Mechanical Engineering*, vol. 52, no. 10, pp. 199–206, 2016.

[19] C. Du, A. R. Plummer, and D. N. Johnston, “Performance analysis of an energy-efficient variable supply pressure electro-hydraulic motion control system,” *Control Engineering Practice*, vol. 48, pp. 10–21, 2016.

[20] K. Baghestan, S. M. Rezaei, H. A. Talebi, and M. Zareinejad, “An energy-saving nonlinear position control strategy for electro-hydraulic servo systems,” *ISA Transactions®*, vol. 59, pp. 268–279, 2015.

[21] J. Zimmerman and M. Ivantysynova, “Hybrid displacement controlled multi-actuator hydraulic systems,” in *Proceedings of the The twelfth scandinavian international conference on fluid power, SICFP11*, pp. 22–27, Tampere, Finland, 2011.

[22] R. Hippalgaonkar and M. Ivantysynova, “A Series-Parallel Hydraulic Hybrid Mini-Excavator with Displacement Controlled Actuators,” in *Proceedings of the 13th Scandinavian International Conference on Fluid Power, June 3-5, 2013, Linköping, Sweden*, pp. 31–42, 2013.

[23] N. Daher and M. Ivantysynova, “Energy analysis of an original steering technology that saves fuel and boosts efficiency,” *Energy Conversion and Management*, vol. 86, pp. 1059–1068, 2014.

[24] M. Sprengel, T. Bleazard, H. Haria, and M. Ivantysynova, “Implementation of a novel hydraulic hybrid powertrain in a sports utility vehicle,” *IFAC-PapersOnLine*, vol. 28, no. 15, pp. 187–194, 2015.

[25] J.-W. Qiao, J.-Z. Shang, X. Chen, Z.-R. Luo, and X.-P. Zhang, “Unilateral self-locking mechanism for inchworm in-pipe robot,” *Journal of Central South University of Technology (English Edition)*, vol. 17, no. 5, pp. 1043–1048, 2010.